The Supplementary Information published with the Advance Article for this paper on 08/11/2023 has been replaced with the current Supplementary Information that includes the addition of the raw data used to calculate the mechanical properties. The raw data contains three sets of data obtained from parallel measurements. The addition of this raw data does not affect the scientific content of the paper.

Supporting information

High-biobased Polymerizable Deep Eutectic Solvents for Sustainable DLP Printing: Assembly Welding and Reprintable Printing

Meiting Liu [a, b], Guixin Zhang [a], Yun Hu [a], Caiying Bo [a], Yan Dai [a], Lihong Hu [a*], Guoqiang Zhu [a*], Yonghong Zhou [a, b]

[a] Co-Innovation Center of Efficient Processing and Utilization of Forest Resources, Key Laboratory of Biomass Energy and Materials, Institute of Chemical Industry of Forest Products, Chinese Academy of Forestry (CAF), Nanjing 210042, China.

[b] College of Chemical Engineering, Nanjing Forestry University, Nanjing 210037, P. R. China

Corresponding authors

* Lihong Hu. E-mail: hlh@icifp.cn; Tel.: +86-(0)25-85482520; Fax: +86-(0)25-85482520.

* Guoqiang Zhu. E-mail: zhuguoqianglh@163.com; Tel.: +86-(0)25-85482520; Fax: +86-(0)25-85482520.

S1 Characterizations

Fourier transform infrared (FTIR) spectra were recorded from 500 to 4000 cm^{-1} using a Nicolet iS10 IR spectrometer (Thermo-Fisher Corporation, USA). Viscosities were measured at 25 °C using a DVS+ digital display viscometer (Brookfield Corporation, USA). The volume shrinkage (ΔV) was measured using a ZMD-2 electronic automatic density meter (Shanghai Fangrui Instrument Corporation, China). The densities of the CDAG-*x* before and after UV-curing (ρ_0 and ρ_c) were measured at room temperature, and ΔV was calculated using the following equation: $\Delta V=(\rho_c-\rho_0)\times100\%/\rho_c$. Real-time IR (RT-IR) tests were conducted using a modified Nicolet 5700 spectrometer (Thermo-Nicolet Instrument Corporation, USA), and C=C conversion was determined by monitoring the intensity of the C=C peak at around 810 cm^{-1}. The transparency of all the samples was determined using a UV-1990i UV-vis spectrophotometer (Shimadzu Corporation, Japan). The light intensity of the UV projection was measured on a UV-A UV irradiation meter (Beijing Shida Photoelectric Technology Corporation, China). Tensile tests were conducted at 25 °C on a 4201 universal testing machine (Instron Corporation, USA), with an extension speed set at 10 mm/min. The bone-shaped test samples (length: 63.5 mm, width: 3.18 mm and gauge length: 9.53 mm) used in the tensile test were UV-cured. The Young's modulus was calculated as the slope of the tensile stress-strain curves. Thermogravimetric analysis (TGA) tests were conducted using an STA 409PC thermogravimetry instrument (Netzsch Company, Germany) at a heating rate of 15 °C•min^{-1} with a N_2 flow rate of 100 mL•min^{-1}. Differential Scanning Calorimetry (DSC) tests were performed using a Polyma NETZSCH scanner (214 Polymer, Germany) at a heating rate of 10 °C•min^{-1} over a temperature range of -50 °C to 100 °C. The surface images of the color plate were captured using a Leica DM750M microscope (Leica Corporation, Germany). Morphological analysis of thermochromic microcapsules was conducted using a S3400N-I scanning electron microscope (HITACHI Corporation, Japan).

S2 CDAG-*x* PDES with different content of Gly

Table S1 Compositions of CDAG samples

Samples	CA (g)	DMAA (g)	AAm (g)	Gly (g)	HQ （g）	TPO-L (g)	C_{bio}
CDAG-10%	19.212	19.826	7.108	4.615	0.253	0.508	46.9%
CDAG-15%	19.212	19.826	7.108	6.922	0.265	0.531	49.2%
CDAG-20%	19.212	19.826	7.108	9.229	0.277	0.554	51.4%
CDAG-30%	19.212	19.826	7.108	13.844	0.300	0.560	55.1%
CDAG-40%	19.212	19.826	7.108	18.458	0.323	0.646	58.3%

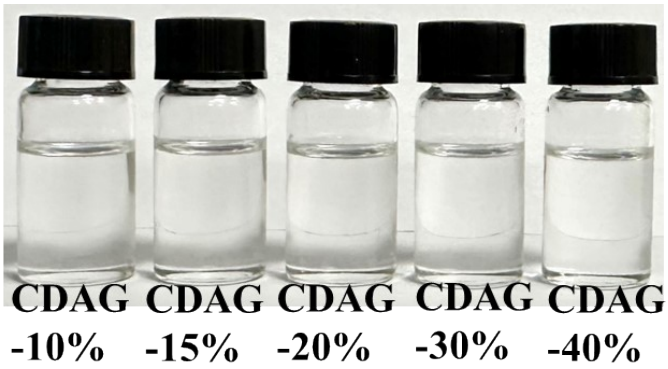

Figure S1 CDAG-*x* PDES with different content of Gly.

S3 FI-IR spectra of DMAA, AAm, Gly, CA and CDAG-15%

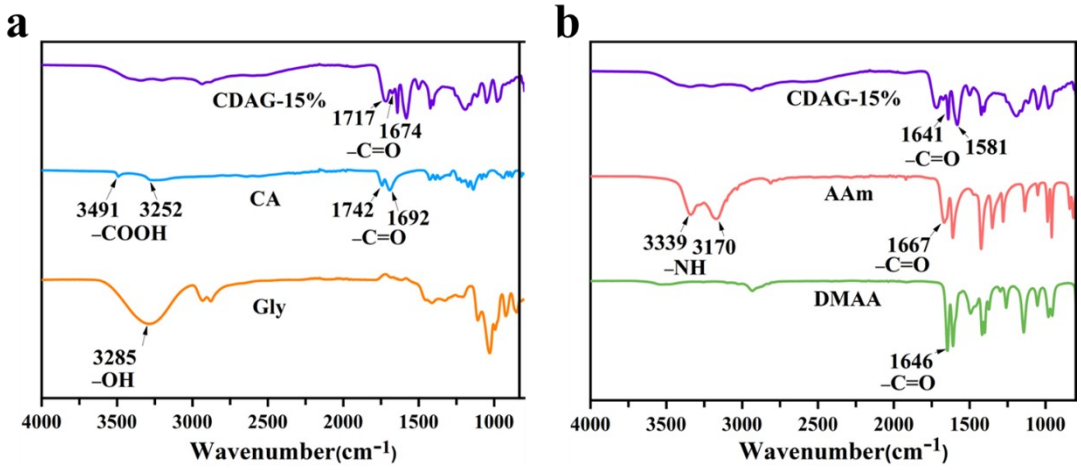

Figure S2 (a) FI-IR spectra of Gly, CA and CDAG-15%; (b) FI-IR spectra of DMAA, AAm and CDAG-15%

S4 DFT calculations of the CDAG-*x* systems

The DFT calculations were carried out with Gaussian 16 software.[1] Only one structural unit was considered to determine weak interactions qualitatively. The optimization of the structures and frequency analysis were performed by using B3LYP-D3 functional with 6-31+G* bases set, and the single point calculation was carried out with higher basis set B3LYP-D3/6-311++G(2df,2p) level. In order to confirm the presence of structure minimum, the frequency calculation was carried out at the same time with structure calculation. The non-covalent interactions were analyzed by the reduced density gradient (RDG). The RDG isosurfaces were plotted with Multiwfn 3.6,[2] vmd,[3] and gnuplot.[4]

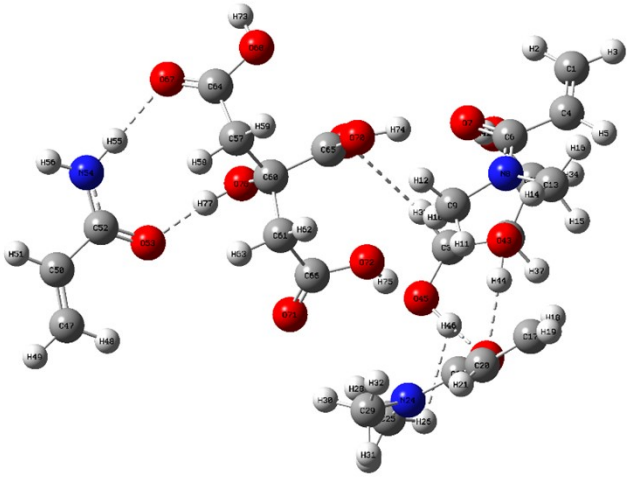

Figure S3 Optimized structures of CDAG-*x*.

S5 MD simulation of the cured CDAG-*x*

The molecular dynamics (MD) simulation was carried on the COMPASSII fore-filed module of Materials Studio package in cubic boxes with periodic boundary conditions for three directions. In general, the COMPASSII force-field is suitable for polymer systems and has been applied in many research systems. Two different types of models were built in the Visualizer module of Materials Studio, including CDAG-15% and CDAG-40%. In this work, the poly(DMAA-AAm) polymer chain was consist of twenty DMAA and ten AAm monomers. Two amorphous molecular models of CDAG-15% and CDAG-40% were built by using Amorphous Cell module. An atom-based method and a cut-off distance of 9.5 Å with the Ewald method were used for calculating Van der Waals and Coulomb forces. When the temperature and energy tended to be constant, the whole dynamic system was considered as the equilibrium state.

Parameters of used amorphous unit cells

Sample	CDAG-15%	CDAG-40%
Initial density (g/m^3)	1.16	1.13
Unit cell size (Å)	32.45	33.7
Number of polymer chain	4	4
Number of CA	40	40
Number of Gly	30	80

Table S2 H-bonds in the cured CDAG-15% and CDAG-40%

Sample	CDAG-15%	CDAG-40%
Range of H-bond length (Å)	1.458~2.498	1.458~2.498
Number of H-bond	465	524
Average H-bond length (Å)	1.94	2.04

S6 MD Viscosity curves of CDAG-*x* with different shear rates.

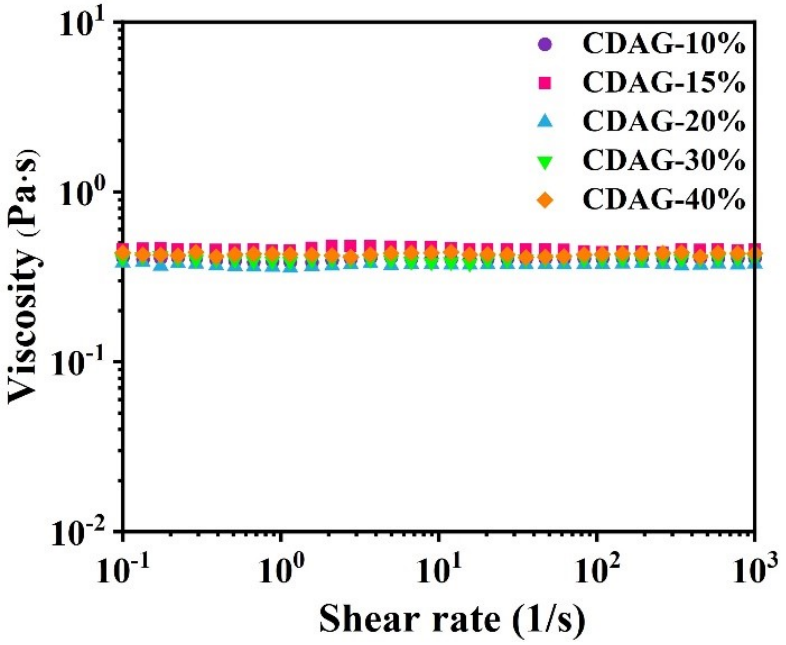

Figure S4 Viscosity curves of CDAG-*x* with different shear rates.

S7 Stress-strain curves of UV-cured CDAG-0% and CDAG-15%

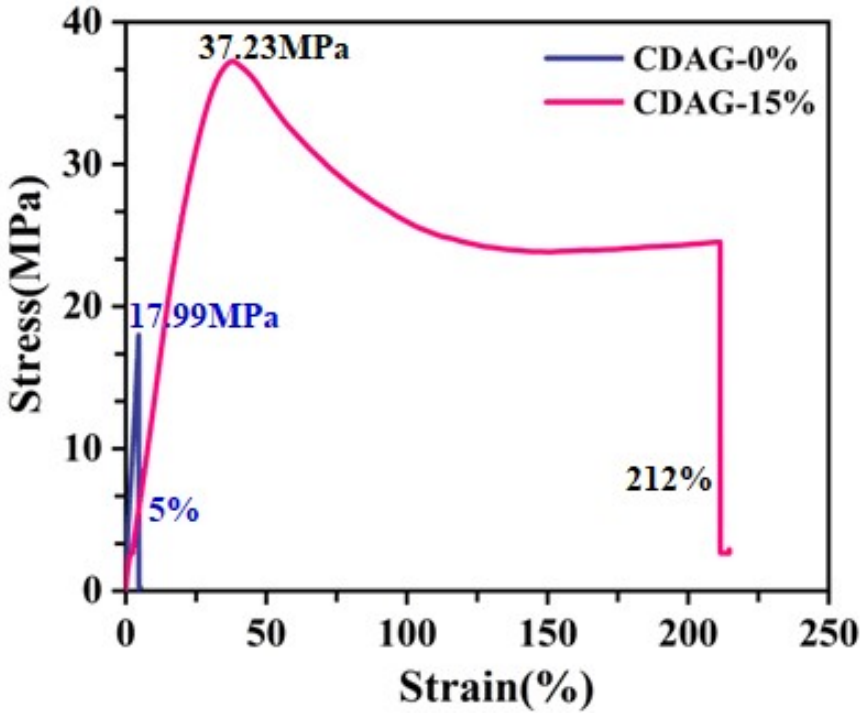

Figure S5 Stress-strain curves of UV-cured CDAG-0% and CDAG-15%.

S8 Self-healing properties.

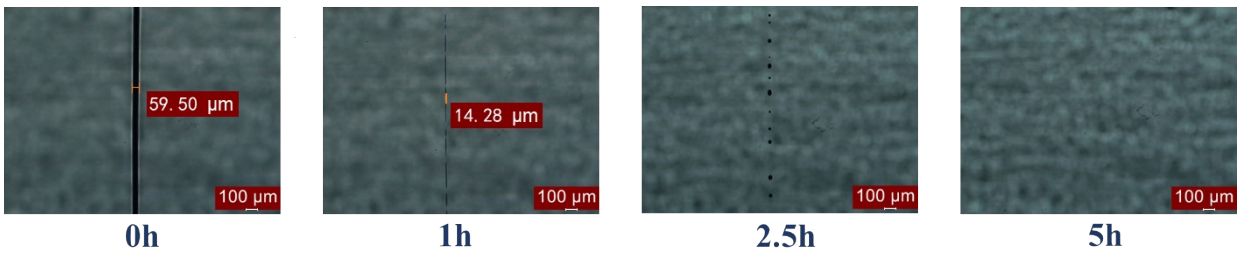

Figure S6 Optical microscope images recorded during the self-healing process of CDAG-15% at room temperature.

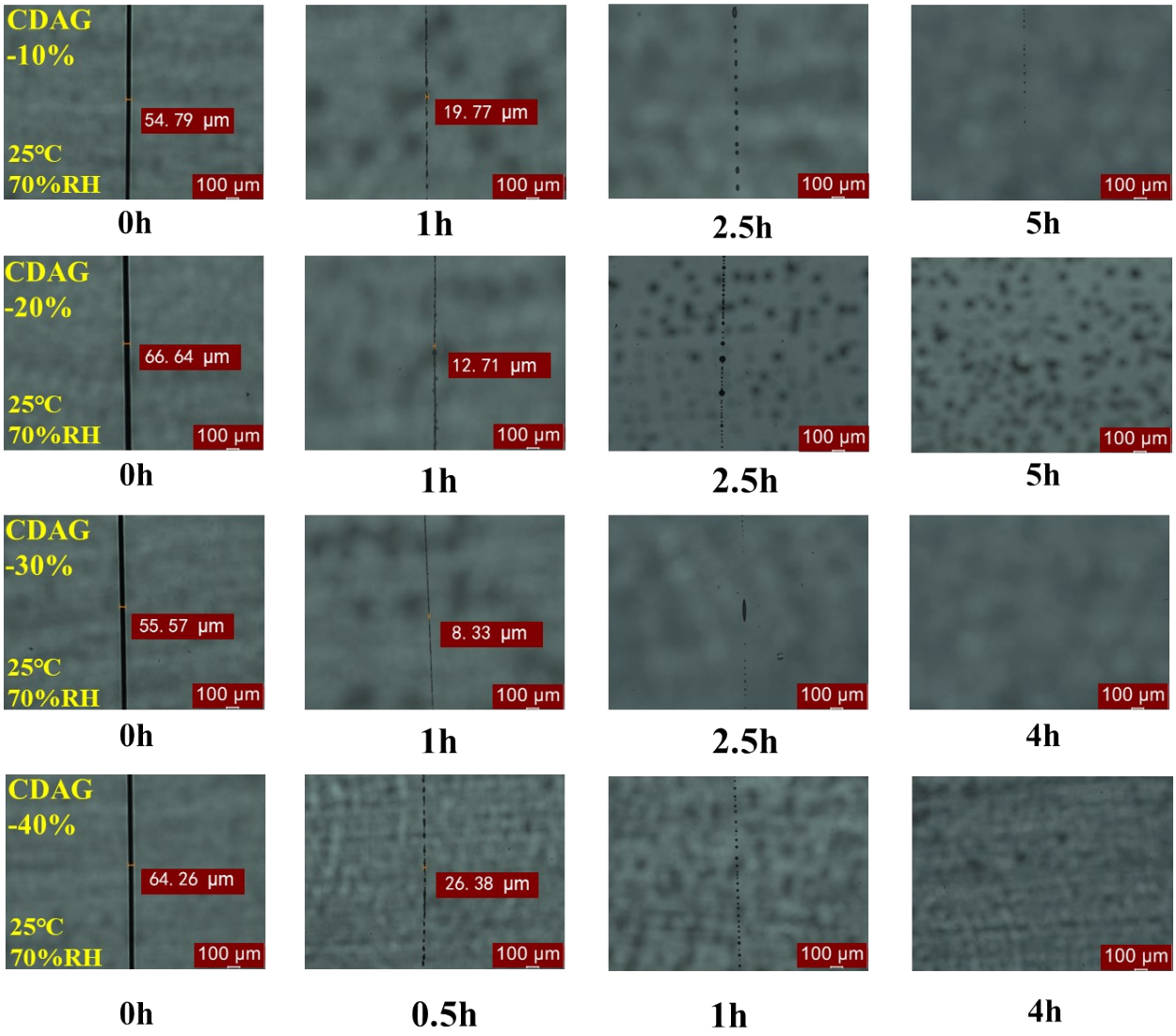

Figure S7 Optical microscope images recorded during the self-healing process of CDAG-*x* at room temperature.

Table S3 Mechanical properties of CDAG-15% sample after healing.

Samples	σ (MPa)	R_e * (%)	E (MPa)	R_e * (%)	ε (%)	R_e * (%)
Original	37.2±0.44	-	144.4±0.87	-	212.1±2.3	-
Healed (3 h)	24.2±0.27	64.9	90.8±0.44	62.9	25.7±0.3	12.1
Healed (8 h)	30.4±0.62	81.7	125.2±1.14	86.7	87.2±0.47	41.1
Healed (12 h)	33.1±0.38	88.9	129.8±0.83	89.9	181.0±1.1	85.3

* Healing efficiency for each property.

S9 CDAG-15% without the addition of a light absorber failed to print.

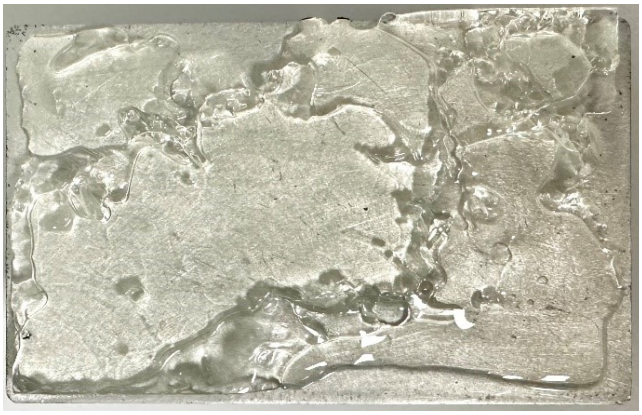

Figure S8 During the printing process of CDAG-15% without the addition of a light-absorbing agent, overexposure occurred.

S10 CDAG-15% recycling and reprinting performance.

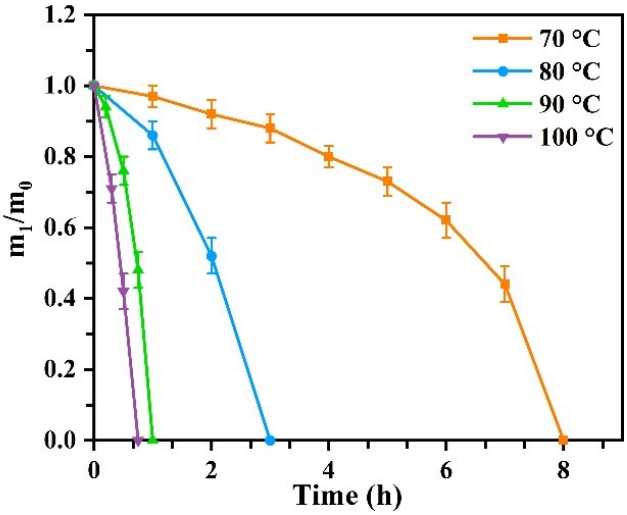

Figure S9 The changes in the mass ratio (m_1/m_0) of the dissolved material to the original CDAG-15% material at different temperatures

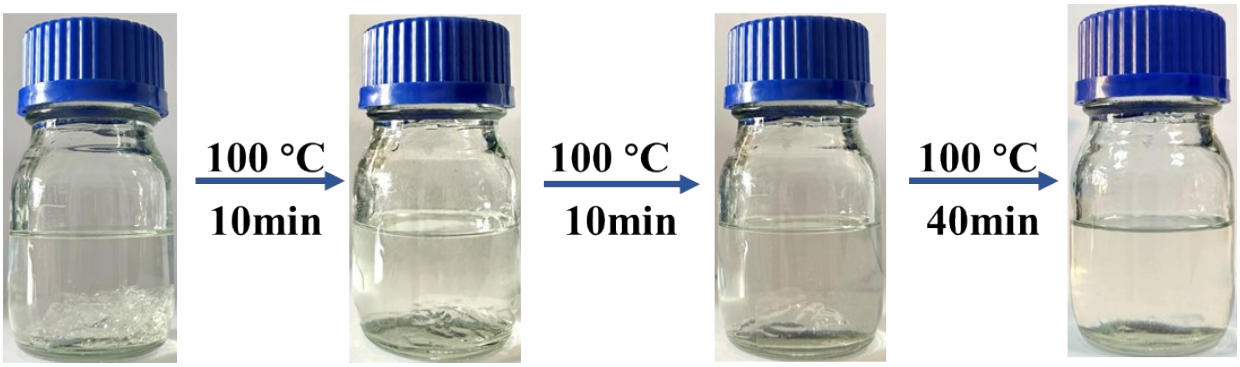

Figure S10 During the printing process of CDAG-15% without the addition of a light-absorbing agent, overexposure occurred.

Table S4 Physical, thermomechanical and mechanical properties of UV-cured CDAG-15% and reprinted CDAG-15%.

Samples	V_s (mPa·s)	ΔV (%)	σ (MPa)	E (MPa)	ε(%)	T_g (°C)	T_i (°C)	w_{char} (%)
CDAG-15%	424±14	6.46±0.17	37.23±0.8	144.35±8	212±7	52.07	196.3	8.4
Reprint CDAG-15%	591±18	6.78±0.08	36.41±0.5	142.13±11	224±11	52.41	196.7	8.33

S11 thermochromic capsules.

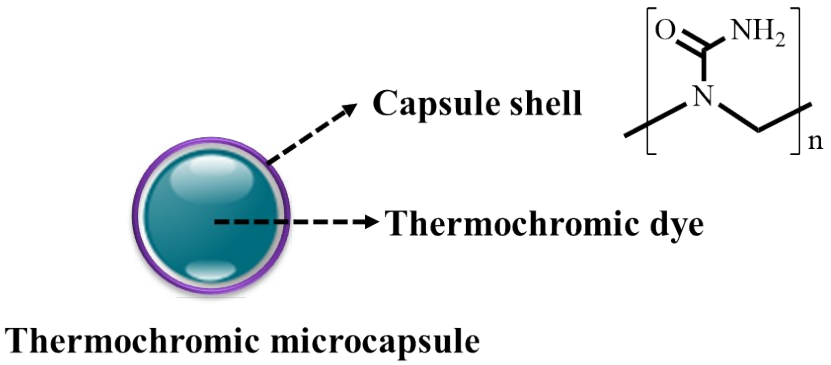

Figure S11 The structure of microcapsules.

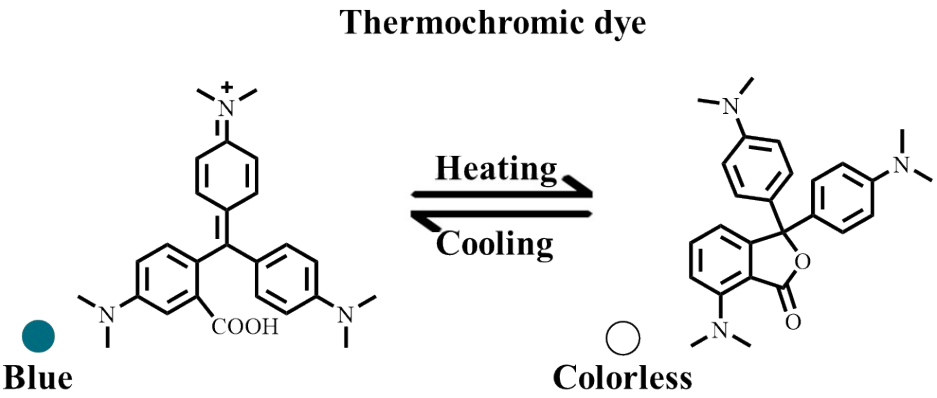

Figure S12 The thermochromic mechanism of thermochromic microcapsules.

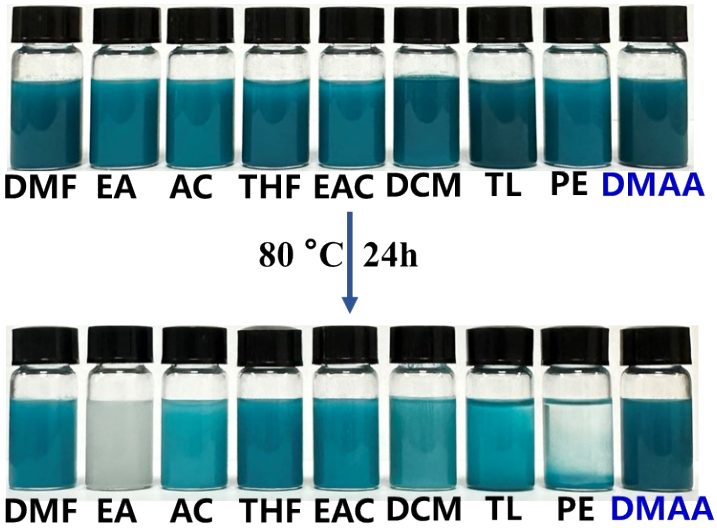

Figure S13 Solvent resistance of blue thermochromic microcapsules in different solvents.

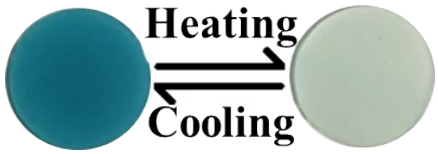

Figure S14 Reversibility of thermochromic properties of materials.

S12 Tensile tests.

Tensile tests were conducted on UV-cured CDAG-15% material to evaluate the mechanical properties of the printed material. The tensile tests were performed using a 4201 universal testing machine (Instron Corporation, USA) with an extension speed set at 10 mm/min and the testing environment was controlled at room temperature (23-25 °C). The rectangular test specimens had dimensions of 80×10×2 mm^3, and the UV intensity and exposure time for curing the test specimens were consistent with those used for post-curing the printed models. It is important to note that we observed significant effects of high temperature and high humidity on the mechanical properties of the CDAG-15% material. Therefore, mechanical performance testing needs to be conducted in a low humidity environment (40-50% RH) at room temperature (23-25 °C), and the raw materials for CDAG-15% preparation require drying treatment.

Reference

1. M. Frisch, G. Trucks, H. Schlegel, G. Scuseria, M. Robb, J. Cheeseman, G. Scalmani, V. Barone, G. Petersson and H. Nakatsuji, *Gaussian 16*, Gaussian, Inc., Wallingford CT, 2016.
2. T. Lu and F. Chen, *Journal of Computational Chemistry*, 2012, **33**, 580-592.
3. W. Humphrey, A. Dalke and K. Schulten, *Journal of Molecular Graphics*, 1996, **14**, 33-38.
4. T. Williams, C. Kelley and etc, *GNUPLOT Version 5.2 patchlevel 6, Copyright 1986-1993, 1998, 2004*, 1998.